Chapter 6

Digital Nucleic Acid Detection Based on Microfluidic Lab-on-a-Chip Devices

Xiong Ding and Ying Mu

Additional information is available at the end of the chapter

http://dx.doi.org/10.5772/62742

Abstract

Microfluidic lab-on-a-chip (LOC) technologies have been developed as a promising alternative to traditional central laboratory-based analysis approaches over several decades due to the capability of realizing miniaturized multiphase and multistep reactions. In the field of nucleic acid (NA) diagnosis, digital NA detection (dNAD) as a single-molecular-level detection is greatly attributed to the perfect combination of NA amplification and microfluidic LOC techniques. In this chapter, the principle, classification, advances, and application of dNAD will be involved. In particular, the focus will be on chip-based dNAD for giving a deep interpretation of the analysis and evaluation of digital detection. The future prospect of dNAD is also anticipated. It is sure that dNAD by means of microfluidic LOC devices as the promising technique will better serve the ambitious plan of precision medicine through absolute quantitation of NA from individuals.

Keywords: digital nucleic acid detection, lab-on-a-chip, microfluidic chip, digital PCR, quantitation

1. Introduction

It has been clearly investigated that nearly all of the diseases possess a series of biomarkers associated with nucleic acid (NA) molecules during the development of biological researches [1–5]. Determining these NA molecules and their intercellular and extracellular changes is a well-worked strategy for estimating therapy efficacy, monitoring minimal residual diseases, unveiling the mechanisms of cellular signal transduction, and so on [6–8]. To reflect individual genetic differences, single-molecule level quantitation of NAs has been increasingly con-

cerned recently due to its superiority on analytical sensitivity and accuracy [9, 10]. Furthermore, single NA molecule detection is also highly preferred as the calibration strategy for next-generation sequencing (NGS) to better serve recently proposed ambitious plans of precision medicine [11–13]. Thus, testing NAs, especially in single-molecule level, plays an essential role in modern biological researches and diagnosis fields.

At present, the widely used approaches in detecting NA molecules are quantitative polymerase chain reaction (qPCR) and quantitative reverse transcription-PCR (qRT-PCR). Apart from the capability of real-time monitoring the amplification, they can be applied to quantify the target NA molecules through two common strategies: relative quantification and absolute quantification. The former is based on internal reference genes (namely, housekeeping genes) to normalize and reflect fold differences in expression levels of mRNA, which is commonly interpreted as cDNA [14, 15]. The latter can provide the exact number of targeted molecules using an established standard curve of the change in quantification cycles with known molecule number of NA standards [16–19]. However, qPCR is compromising the ability of single-molecule quantitation analysis [20, 21]. Alternatively, when PCR meets microfluidic or nanofluidic chips, a highly sensitive NA quantification technique [digital PCR (dPCR)] emerges, estimating NAs advantageously at a single-molecule analysis level [22].

At the end of 20th century, the first concept of dPCR was proposed by Vogelstein and Kinzler [23]. Since the concept was proposed, many dPCR platforms have been launched for several

Figure 1. Some vendors and their launched microfluidic chips and dPCR devices. The pictures are all from the websites of the corresponding companies or reprinted with permission from Ref. [59]. © Copyright 2011 American Chemical Society.

http://dx.doi.org/10.5772/62742

decades based on differently designed microsystems, including femtoliter array, spinning disk, SlipChip, droplet, microfluidic formats, and so on [24–30]. Some even have been successfully paced into industrial phase because of the superiority of testing and the promising application. Currently, several vendors in the biological industry, such as Fluidigm, Bio-Rad Laboratories, Life Technologies (ThermoFisher), RainDance Technologies, and Formulatrix, have launch individually their commercialized dPCR devices (**Figure 1**).

Apart from dPCR, digital isothermal NA amplification (dINAA) devices also arouse great concern. Unlike dPCR, dINAA leans on the isothermal NA amplification, which can be carried out at a consistent temperature, obviating the requirement of highly stable thermocycling devices. Thus, when targeting practical point-of-care testing (POCT) devices, dINAA is superior to dPCR. However, viewed from the principle of realizing digital detection, the concept of dINAA is the same as that of dPCR, just replacing PCR with isothermal amplification. In particular, due to loop-mediated isothermal amplification (LAMP) displaying as the best promising method among a lot of isothermal NA amplifications, digital LAMP (dLAMP) is the first dINAA developed [31, 32]. Later, other dINAAs have been reported, such as digital multiple displacement amplification (dMDA), digital isothermal multiple-self-matching-initiated amplification (dIMSA), digital recombinant polymerase amplification (dRPA), and so on [33–38]. However, the development of dINAA devices is still in the research stage, as the commercial products have not been launched yet.

As of now, more and more researchers are enthusiastic about the potential of digital NA detection (dNAD) based on microfluidic Lab-on-a-Chip (LOC) devices, since an increasingly significant role has been played in single-cell analysis, early diagnosis of cancer, prenatal diagnosis, and so on. In this chapter, we will concentrate on the principle, classification and advances, analysis and evaluation, application, and future prospects of dNADs that are accomplished either through commercialized LOC devices or the devices our laboratory or other laboratories have established.

2. Principle of dNAD

According to the strategies of amplifying NA, dNAD or single-molecule NA detection can be divided into dPCR and dINAA. However, both of them share the same principle.

Generally speaking, the principle of dNAD is composed of three core steps [39]. First, the original sample should be partitioned into thousands or hundreds of thousands of individual microreactions, endeavoring to make each contain nearly one target molecule. Second, the number of "positive" microreactors indicated either in a real-time reaction or in an endpoint reaction is counted and analyzed. Third, the concentration of nonpartitioned sample is calculated using certain statistical methods. In theory, if the number of microreaction is more enough or the number of target molecules is less enough, one reaction unit with positive signal represents one target molecule. However, in fact, a positive partition may contain more than one molecule. Therefore, in calculating the target's true concentration, a Poisson distribution is adopted in hope to correct the results. Therefore, dNAD can be considered as a binary output (present or absent like "1" or "0" in computer science) measurement, giving a direct and high-

confidence NA molecule's measurement method [10, 40]. Compared to conventional tube-based NA detection, digital analysis is superior in realizing the absolute quantification with high sensitivity, high precision, and low ambiguity, avoiding the requirement of establishing a standard curve.

3. Classification and advances of dNAD

In the early stage of digital detection, the used materials are 96- and 384-microwell plates. Then, due to the rapid development of microfluidic chip techniques, an increasing number of digital detection devices emerge. Also, a variety of materials have been used individually or jointly, such as silicon wafer, quartz, glass, polydimethylsiloxane (PDMS), polymethyl methacrylate, and so on. According to the approaches to partition reaction mixture, the currently launched dNAD methods can be roughly grouped into three categories: plate-based dNAD (pdNAD), droplet-based dNAD (ddNAD), and chip-based dNAD (cdNAD). On structural design, each classified dNAD has the advantages and disadvantages, and the corresponding commercial devices are also developed. In this subchapter, we are going to narrate their features and recent advances in either commercial or research aspects.

3.1. pdNAD

At present, most of the pdNADs are established as dPCR devices, but they are not hard to be developed as dINAA platforms. As the first generation of dNAD, plate-based dPCR (pdPCR) was first conducted using plenty of commercially available 96- and 384-microwell plates [23, 41]. The biggest benefit for this kind of digital platform is saving to create the plates that have been widely used in conventional PCR. Each microwell undertakes each microreaction; therefore, the high sensitivity and accuracy of detection lean entirely on the enough number of microwells. However, actually, the number is hard to be reached just using microwell plates.

Another problem causing the embarrassment is the volume of reagents required [42]. For each microwell, more than 5 μL are needed, and the cost of reagents inevitably daunts most researchers, let alone the application for POCT. To break the barriers, some researchers made modification. As shown in **Figure 2**, Morrison et al. deceased the volume of microreaction into 33 nL using a stainless steel plate (25 mm in width and 75 mm in length) in which up to 3072 microholes (320 μm in diameter) were created [43]. In contrast, the required volume was reduced to 1/64, and the throughput was increased by 24-fold, although it had the comparable sensitivity to the past. At present, this technique has been applied to commercial devices in 2009, the OpenArray RealTime PCR System from Life Technologies. However, as the number of reaction units increases, the problem turns into how to efficiently load the reagents. Consequently, it has to use some ancillary equipment-like microarray spotter or mechanical arms, which in turn raises the cost and is cumbersome.

Considering the embarrassing situation, in the second half of 2013, Life Technologies launched the next-generation digital detection device, the QuantStudio 3D dPCR system [42, 44]. It is a simple and affordable platform to provide the reliable and robust dPCR. The device used a

http://dx.doi.org/10.5772/62742

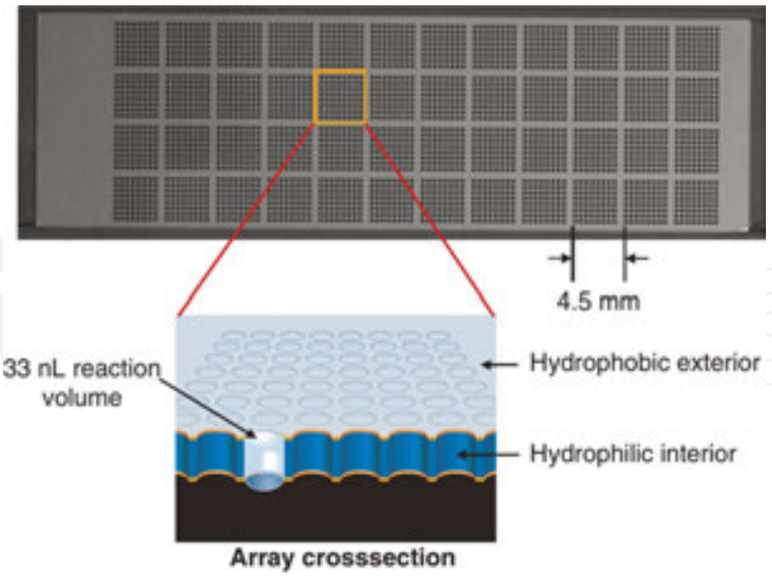

Figure 2. Plate-based chip used for the OpenArray RealTime PCR System. A rectilinear array of 3072 microholes with 320 μm in diameter was fabricated in a stainless steel plate (25×75×0.3 mm). The volume of each hole was approximately 33 nanoliers, and to match the pitch of the wells in a 384-well microplate, the 48 groups of 64 holes are spaced at 4.5 mm. Reprinted with permission from Ref. [43]. © Copyright 2006 Oxford University Press.

special plate (10 mm in width and 10 mm in length) where a total of 20,000 hexagonal microwells are fabricated. The volume of each microwell is 0.8 nL, and each reaction well is isolated absolutely from its neighbors. At present, the system has been applied to the absolute quantification of viral load, low-level pathogen detection, sensitive genetically modified organism (GMO) detection, differential gene expression, copy number variation (CNV), NGS library quantification, and rare mutation analysis [45–50]. Although the cost of reagents is reduced, the system still calls for supporting instruments to load the reagents, amplify the sample, and read the results.

For high-throughput sample analysis, 96- and 384-microplate formats are still of use. Formulatrix introduced a new commercial high-throughput pdPCR device termed as constellation dPCR. The device brings the digital analysis to a 96-sample microplate format, and the so-called high-throughput results from the preformation of dPCR on 96 samples at once and up to 384 samples per hour. As required, the number of partitions for each microwell in the plate can be easily increased, and it reaches 496 for the 96-microplate format.

3.2. ddNAD

ddNAD can go back to emulsion PCR (ePCR) [51–54]. ePCR is widely used for NGS (**Figure 3**) [55]. After generating a DNA library, the fragments of genomic DNA are attached to the beads, because their surface is modified with oligonucleotide probes whose sequences are complementary to the sequences of the fragments. When the beads are compartmentalized into water (the PCR reagent)-oil emulsion droplets, plenty of microreactors are produced. Since each bead captures single-stranded DNA fragment, in theory, ePCR can amplify it down to one DNA molecule. However, it is not easy to partition the fragments and beads into one

droplet simultaneously, and then the performance of ePCR suffers from variety. Benefitting from the rapid development of microfluidic LOC techniques, ddNAD also enjoys a huge boom in recent years. dPCR is still the main part in ddNAD, but droplet-based dINAAs including dLAMP, dRPA, digital rolling circle amplification (RCA), and digital hyperbranched RCA (HRCA) are showing up more and more [34–37, 56].

Figure 3. ePCR used for NGS. Top left: The genomic DNA is isolated, fragmented, ligated to adapters, and separated into single strands. Top right: Fragments are bound to beads that are captured in the droplets of a PCR mixture-in-oil emulsion. Then, ePCR occurs within each droplet. Bottom right: After breaking emulsion and denaturing the DNA strands, beads with single-stranded DNA are deposited into wells of a fiber-optic slide. Bottom left: Pyrophosphate sequencing is initiated within each well after depositing smaller beads carrying immobilized required enzymes. Reprinted with permission from Ref. [55]. © Copyright 2005 Nature Publishing Group.

Beer et al. successfully created picoliter-scale water-in-oil droplets by using a shearing T-junction in a fused-silica device in 2008 [57]. The NA used for the device was RNA; therefore, an off-chip valving system was integrated to stop the droplet motion, because a different thermal cycling was required for reverse transcription and subsequent PCR amplification. Each droplet contained the PCR mixture of single-copy template, primers, and reaction buffer, which was really termed as digital detection. One year later, Mazutis et al. developed a method for high-throughput dINAA platform in a 2 pL droplet-based microfluidic system [35]. The isothermal HRCA was used to perform the DNA amplification in droplets. This platform was demonstrated to allow fast and accurate digital quantification of the template. In 2011, Zhong et al. reported another picoliter-scale droplet-based multiplexing dPCR platform, breaking the one target per color barrier of qPCR [58]. The number of droplets generated reached more than 10^6, which was enough for enhancing the likelihood that only one DNA molecule was amplified in each droplet. Given its great potential in application, RainDance Technologies launched the commercial digital detection system with the highest droplet throughout, the RainDrop dPCR system. Unfortunately, the system may consume up to 50 μL reagents per

http://dx.doi.org/10.5772/62742

sample. Considering this point, the system may be not proper for rare sample detection. At the same year, Hindson et al. also established a high-throughput droplet-based dPCR (ddPCR) platform [59]. A total of 2 million droplets were generated, and the droplets were then transferred into a 96-well plate for TaqMan probe-based PCR. Finally, to read out the results, a flow cytometry-like double-channel fluorescence detection device was used in a microfluidic chip, in which droplets went through one by one. The platform was confirmed to realize the accurate measurement of germ-line CNV, discriminate the mutant molecules from the wild molecules with 10^5-fold excess, and absolutely quantify circulating fetal and maternal DNA from cell-free plasma. Based on the platform, the first commercial ddPCR system was launched by QuantaLife in 2011, but in the end of that year Bio-Rad Laboratories purchased the company and launched the QX100 ddPCR. Recently, the new version, QX200 ddPCR system, is also available.

Apart from the process of droplet generation and subsequent NA amplification, other approaches to generate droplet are also reported. As shown in **Figure 4**, Shen et al. described a SlipChip to create droplet array [26]. The SlipChip was composed of two glass plates, in which elongated wells were designed to overlap and form the fluidic path for reagent loading. After sample loading, the simple slipping of the two plates broke the path, removing the overlap among wells and generating 1280 droplet array (2.6 nL for each). The device had a reservoir preloaded with oil, so each microreactor was absolutely isolated from each other

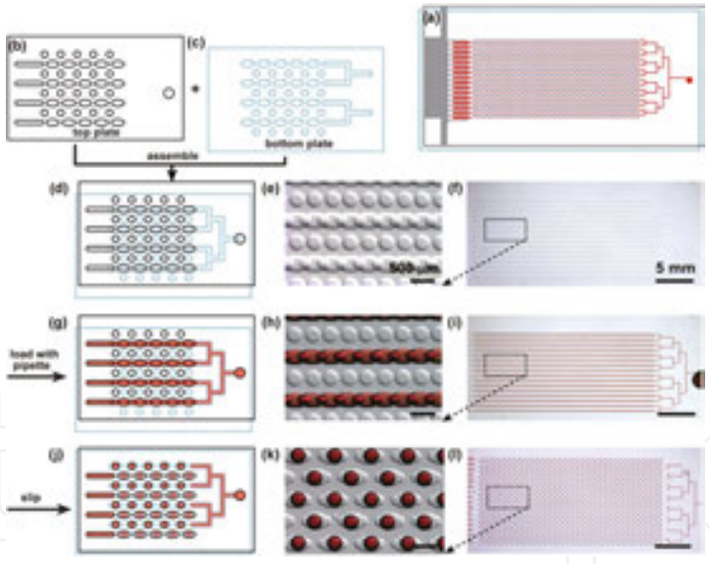

Figure 4. Design and mechanism of the SlipChip for dPCR. The top plate is outlined with a black solid line, the bottom plate is outlined with a blue dotted line, and red represents the sample. (a) Schematic drawing shows the design of the entire assembled SlipChip for dPCR after slipping. (b) Schematic drawing of part of the top plate. (c) Schematic drawing of part of the bottom plate. (d–f) The SlipChip was assembled such that the elongated wells in the top and bottom plates overlapped to form a continuous fluidic path. (g–i) The aqueous reagent (red) was injected into SlipChip and filled the chip through the connected elongated wells. (j–l) The bottom plate was slipped relative to the top plate such that the fluidic path was broken up and the circular wells were overlaid with the elongated wells, and aqueous droplets were formed in each compartment. (d, g, and j) Schematic of the SlipChip. (e, h, and k) Zoomed-in microphotograph of the SlipChip. (f, i, and l) Microphotograph of the entire SlipChip. Reprinted with permission from Ref. [26]. © Copyright 2010 Royal Society of Chemistry.

during thermal cycling. Finally, the results were read out using endpoint fluorescence intensity. The biggest advantage of SlipChip is the capability of realizing multistep manipulation of plenty of microvolumes to form droplet array in parallel. Attributed to the remarkable feature, until now, the SlipChip has been applied to perform immunoassays, protein crystallization, multiplex PCR, dPCR, dLAMP, dRPA, and so on [26, 34, 60–64].

To make the droplet more stable and to easily collect the amplified products, Leng et al. invented an agarose droplet-based single-molecule ePCR device [51]. The agarose performed the unique thermoresponsive sol-gel switching property, and a microfluidic chip was designed to produce uniform agarose solution droplets. Schuler et al. applied centrifugal step emulsification to the fast and easy generation of monodisperse droplets [37]. Only by adjusting the nozzle geometry (depth, width, and step size) and interfacial tensions droplets with desirable diameters could be produced. Using this droplet device, dRPA was successfully established for the absolute quantification of *Listeria monocytogenes* DNA concentration standards within 30 min.

In ddNAD, the microreactors are generated by carefully titrating emulsions of water, oil, and chemical stabilizer; therefore, there is no requirement of the walls of microwells to separate the microreactors. Compared to pdNAD, ddNAD can easily achieve higher throughput via a microdroplet generator to produce hundreds of thousands of droplet reactions per sample. However, the workflow of ddPCR is complicated, referring to generating droplet, transferring droplet, sealing microplate, conventional PCR, and reading out the signal by other devices.

3.3. cdNAD

The development of cdNAD is greatly attributed to the rapid progress of microfluidic techniques, which can realize the low cost, low volume, and high-throughout paralleled NA detections. In the last several decades, microreactors in cdNAD are mainly formed either by the mechanical compartmentalization of PDMS or by the succeeding isolation via immiscible liquid phase. In particular, for PDMS-based chips, the establishment of multilayer soft lithography (MSL) techniques developed by Unger et al. in 2000 also gives a huge boost, making the high-density microwells, micropumps, and microvalves easily fabricated [65]. Based on different power sources to partition reagents, cdNAD can be divided into three categories: integrated fluidic circuit (IFC) cdNAD, self-priming compartmentalization (SPC) cdNAD, and localized temporary negative pressure (LTNP)-assisted cdNAD as well as other cdNADs.

3.3.1. IFC cdNAD

The outstanding feature of IFC chip is the special design of separated and interlaced liquid and gas channels, as shown in **Figure 5**. Taking advantage of the high elasticity of PDMS, hundreds or thousands of microreaction units are formed rapidly when gas channels are added with pressure.

In 2006, Ottesen et al. used the IFC chip to achieve dPCR analysis [66]. A total of 1176 microreaction units were produced by controlling accurately the integrated microvalves and

http://dx.doi.org/10.5772/62742

Figure 5. An IFC chip-based 12×765 digital array from the Fluidigm. Left: Schematic diagram of a part of the IFC chip in which microchambers were connected and isolated by fluidic channels and pressure lines. Right: Optical microscopic images of the part. Reprinted with permission. © Copyright 2009 Springer.

removing the conventional microarray spotter and plates. Now, the IFC chip-based dPCR (IFC cdPCR) platform is successfully established for commercial purpose by Fluidigm. As the first vendor to commercialize dPCR device, Fluidigm provides two IFC-based systems, the BioMark HD and EP1 systems. In the two systems, the PCR reagents are mixed and partitioned automatically, the thermocycling is integrated, and the results can be read out after reaction. The BioMark HD system can offer real-time detection for each tiny reaction and eliminate false positives according to the data, so the system is also available to qPCR. Compared to BioMark HD, EP1 is just an endpoint detection machine, giving the binary output-like data whether or not the microreaction occurs. Recently, Fluidigm also combines with Olink to detect human protein biomarkers based on proximity extension assay (PEA) technology. Until now, the dPCR device from Fluidigm has been applied to single-cell analysis, early diagnosis of cancer, and prenatal diagnosis.

In 2011, Heyries et al. developed a megapixel dPCR platform in which 10^6 microunits were fabricated, and the microreaction's volume reached down to 10 pL (**Figure 6**) [67]. The density of the microreactors reached up to 440,000/mm^2, which was the highest density for IFC platform. On detection performance, this device was able to discriminate one mutant molecule from 10^5 wild molecules and achieve the discrimination of a 1% difference in chromosome copy number. After the platform, in 2012, Men et al. published anther dPCR platform possessing the lowest volume (36 fL) of microreactors until now. Its density of microreactors was more than 20,000/mm^2 [24]. After loading the reagents into all microreactors simultaneously, the deformation of a PDMS membrane was used to completely seal the filled microreactors. Due to the femtoliter-level microreactors fabricated, the device can greatly reduce the consumption of reagent and sample.

Figure 6. Schematic of megapixel dPCR device (a) and the layered device structure (b). Reprinted with permission from Ref. [67]. © Copyright 2011 Nature Publishing Group.

For dINAA, IFC chip is also combined with isothermal MDA to develop dMDA for enumeration of total NA contamination [33]. On detection of microbial genomic DNA fragments, dMDA performs higher sensitivity with orders of magnitude than qPCR.

By making the microchamber smaller or increasing its number, IFC cdNAD has a potential to be developed into a digital detection platform with higher throughout, higher density, and higher discrimination ability, but this platform still relies on the control system of integrated microvalves and micropumps to load and partition the reagents, which is hard to be applied towards POCT. Furthermore, narrowing the size of microchamber endlessly may have an impact on the efficiency of NA amplification.

3.3.2. SPC cdNAD

Targeting practical POCT devices, currently proposed plate-based, droplet-based, and IFC cdNADs are confronted with the huge challenge of demand for peripheral control instrument, for instance, external syringe pumps, droplet generation devices, and plenty of integrated microvalves and micropumps. Upon this challenge, the built-in power-driving, self-partitioning, easy-to-use, and low-priced SPC cdNADs were developed by our laboratory. The built-in power results from the gas solubility and permeability of PDMS, because PDMS remains absorbing gas and letting gas go through them, although PDMS is in a solid state in chips [68].

The chip possesses the prominent feature of SPC, resulting from the used material of silicone elastomer PDMS, a relatively cheap material, which possesses high gas solubility and permeability. When the fabricated chips are evacuated, a negative pressure environment is formed due to the gas solubility of PDMS, which can service as a self-priming power to let the sample solutions be sucked into each reaction chamber and sequentially the biocompatible oil to seal and separate each filled chamber. Thus, in realizing dNAD, thousands of independent microwells can be created automatically, avoiding the external control system, which is superior to IFC cdNAD. Currently, SPC cdPCR and dINAAs [SPC chip-based dLAMP

(cdLAMP) and SPC chip-based dIMSA (cdIMSA)] have been developed by our laboratory [30, 31, 69, 70].

3.3.2.1. SPC cdPCR

The chip shown in **Figure 7** is composed of three PDMS layers, two glass coverslips, and a waterproof layer [30]. The three PDMS layers include an inlet and outlet layer, a microwell array layer, and a blank layer. In the microwell array layer, a total of 5120 reaction microwells (150 μm in width, 150 μm in length, and 250 μm in height) are equally distributed in four separate panels. Each microwell contains down to 5 nL solution. The inlet and outlet layers have four 0.5-mm holes and four 2.5-mm holes in diameter punched as injection ports and suction chambers when aligning to the outlet of the microwell array layer, respectively. For mechanical stability, the blank layer coats the microwell array layer with the waterproof layer embedded. The waterproof layer is made of low permeability fluorosilane polymer, which beneficially prevents the evaporation during the step of denaturing template DNA at 95°C in PCR. One of the glass coverslips with plasma pretreated are used to seal the microwell array, and the other one is pressed on the upper surface of the SPC chip for mechanical stability at the end of microchip operation.

MSL techniques are used to fabricate the SPC chip. The chip patterns are designed by a software of CorelDRAW X4 and printed on transparency films using a high-resolution printer to create

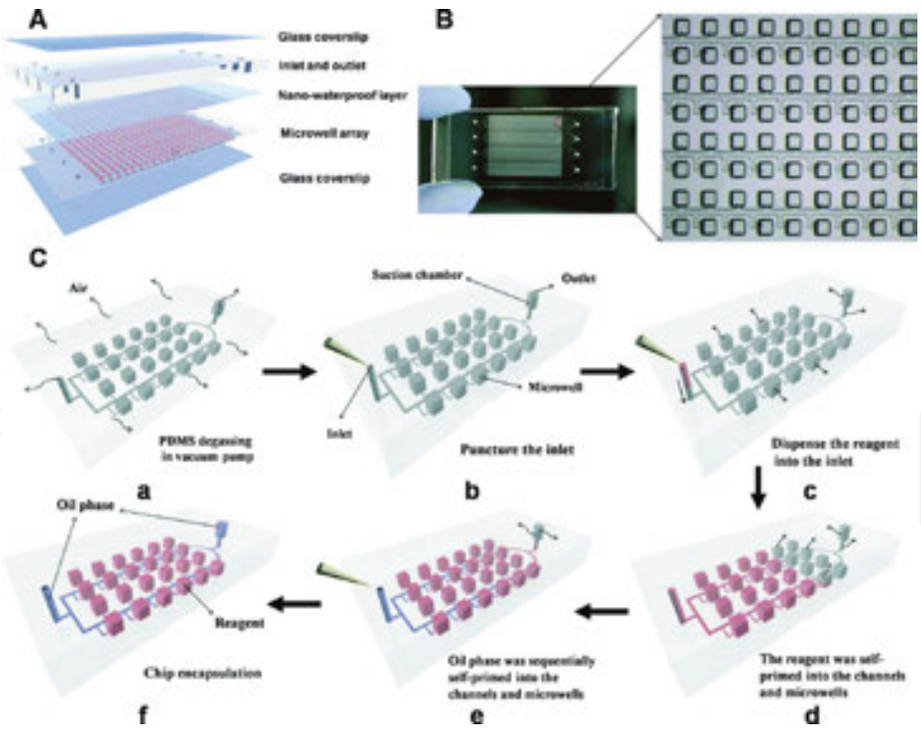

Figure 7. (A) Schematic diagram of the layered device structure of the SPC chip. (B) Photograph of the prototype SPC cdPCR device. The size of the chip is 50×24×4 mm. (C) Principle and operation procedure of the SPC microfluidic device. The red cuboids (150×150×250 μm) stand for the microwells. Reprinted with permission from Ref. [30]. © Copyright 2014 Royal Society of Chemistry.

the masks of channels and microwells. The photoresist material used are SU8 serials, which are a high-contrast, epoxy-based negative photoresist. Several 4-inch silicon wafers are adopted as the mold substrate. The PDMS to replicate the SPC chip is the silicone elastomer PDMS, which is composed of PDMS base (A) and catalyst (B) at certain ratios. Because dPCR is an endpoint detection, the reaction components including PCR buffer, primers, labeled probes, and templates have to be mixed before loading into the chip. Each diluted template in the mixture is individually injected into the three panels of the chip, allowing the samples to be compartmentalized completely and each chamber contains down to 5 nL solution. A Maestro Ex In-Vivo Imaging System (CRI Maestro, USA) is used to capture the fluorescent image of the microchip after dPCR. As a new generation of microfluidic chips, SPC cdPCR has been successfully applied to the absolute quantification of β-actin DNAs and the lung cancer-related genes.

3.3.2.2. SPC chip-based dINAAs (cdINAAs)

Although PCR is widely adopted and used as a standard analytical technique in molecular diagnosis, it is remarkably confined when applied to field and POCT due to the facts that it requires nonportable thermocycling facilities, its process of obtaining results is cumbersome, and the whole amplification takes 2 h or more. Also, SPC cdPCR confronts the same defects. Accordingly, SPC cdLAMP and SPC cdIMSA are established by our laboratory. As simple and easy world-to-chip fluidic devices, SPC cdINAAs have the great potential in POCT for the developing countries.

Similar to SPC cdPCR, SPC cdLAMP is also the completely valve-free and SPC device (**Figure 8**) [31]. It is also made mainly of PDMS and fabricated by MSL techniques. In size, the SPC chip used for dLAMP is the same as the dPCR-used chip; however, in composition, it does not contain a waterproof layer because of the absence of the DNA denaturing step in LAMP. For the microwell array PDMS layer of dLAMP-used SPC chip, a total of 4800 microwells (150 μm in width, 150 μm in length, and 300 μm in height) are fabricated and they are also equally distributed into four panels (each contains 1200 chambers), and the interval for two closed chambers is 150 μm. The big difference from the dPCR-used SPC is that the rectangular chambers are located vertically on the main channels and the branch channels link to chamber without orthogonal turning points. On performance, the SPC cdLAMP can precisely calculate the absolute DNA concentration. To conduct the data acquisition and analysis of SPC cdLAMP, the Maestro Ex In-Vivo Imaging System is employed. However, the imaging system is too cumbersome and expensive to allow the e POCT, especially in the less developed regions. Herein, an easy-to-use and cost-efficient smartphone-based dLAMP POCT device platform is also established by our laboratory.

SPC cdIMSA is an updated version of SPC cdLAMP, in which the LAMP is replaced by IMSA and a mixed dye is used to establish a label-free and sensitive dual-fluorescence detection for on-chip IMSA [70, 71]. The used SPC chip for dIMSA is the same as that for dPCR without any modifications. The SPC cdIMSA with the mixed dye for the detection of hepatitis B virus (HBV) is conducted. In contrast, the mixed dye indicating two different colors makes it easy to count the positive chamber number by visual inspection regardless of the cutoff values. Also, there

http://dx.doi.org/10.5772/62742

Figure 8. (a) Schematic diagram of the SPC chip for cdLAMP. (b) Schematic of the whole microchip and the enlarged schematic diagram of the part of the chip, with insets showing the array and microwell geometries. It contains four separate panels, each of which has an individual inlet and outlet. The blue lines (8×50 μm) are the flow channel. The red spots (150×150×300 μm) stand for the microwells. Each microwell was partitioned by oil. (c) Photograph of the prototype SPC cdLAMP device. Reprinted with permission from Ref. [31]. © Copyright 2012 Royal Society of Chemistry.

is a linear response of the counted positive chamber number to the dilution ratios of templates. Moreover, the dual fluorescence is capable of indicating more positive chamber number in contrast to single fluorescence by SYBR Green I. The mixed dye-loaded SPC cdIMSA possesses the advantage of enlarging the color changes over other currently used dyes or indicators. Similarly, the mixed dye-based dual-fluorescence detection has a potential in the POCT application of SPC cdLAMP and other SPC chip-based dINAAs.

3.3.3. LTNP cdNAD

As another POCT-oriented LOC device, LTNP chip resembling SPC chip also uses the gas solubility of PDMS to load solution into chambers (**Figure 9**) [29]. However, the measure of evacuating the LTNP chip is different from the SPC chip. For the former, the gas solubility and permeability of the chip itself and another PDMS layer coating on the chip services simultaneously as the real-time power source of evacuating with a syringe filter. For the latter, preevacuating by a vacuum pump is indispensable, which calls for robust and efficient approaches of sealing and packaging chips [30].

The LTNP cdPCR has been already exploited [29]. The chip consists of three parts, which are a lamina-chip layer (LCL), a vaporproof layer (VPL), and a syringe filter-like microfluidic device (μfilter) with helical channels. The μfilter has two parts. One is designed for generating the LTNP through pulling the plug of the syringe connected at one end of helical channels. The helical channel in the μfilter is 200 μm in width and 40 μm in depth. The other is used for

sample and oil loading via the punched ports (0.5 mm in diameter) aligning at the ones in the LCL. The area diameter of the region of helical channel in the two μfilters is 20 mm, covering entirely the area of the whole chambers in the LCL. Sandwiched by the two parts of the μfilter, LCL contains 650 chambers in a square array. The chamber is cylindrical with 200 μm in diameter and 200 μm in depth, and the distance between two closed chambers is also 200 μm. VPL on the LCL is also a thin circular layer with chambers at 100 mm in diameter, and its area is 17.0 mm in diameter, entirely mulching the LCL.

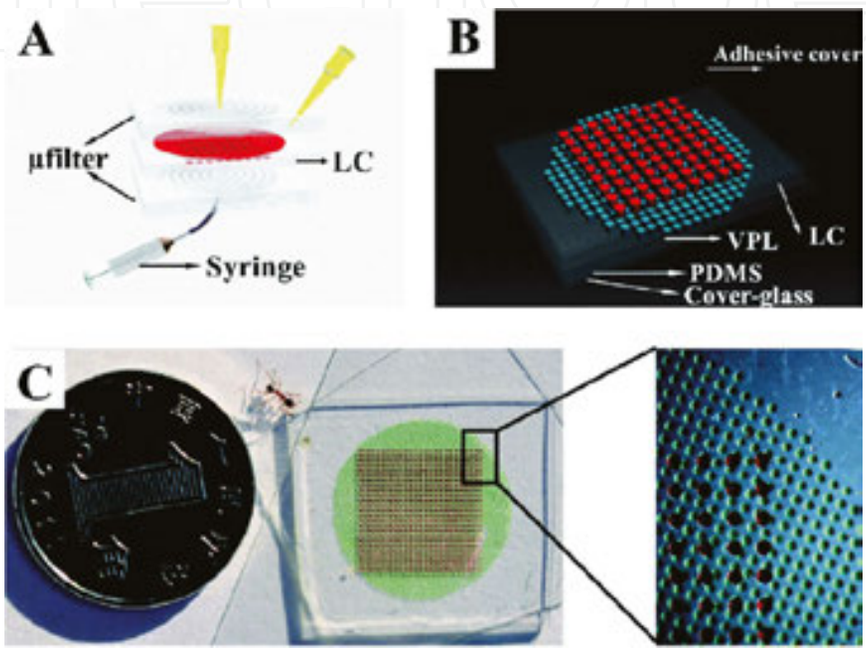

Figure 9. (A) Schematic diagram of the LTNP chip. (B) Schematic of the reagent-loaded chip. It contains reagent-loaded lamina chip (red), water-loaded VPL (blue), PDMS on the coverglass, and optical adhesive cover. (C) Digital image of the prototype LTNP cdPCR device. Reprinted with permission from Ref. [29]. © Copyright 2015 Royal Society of Chemistry.

Currently, LTNP cdPCR has been used for the detection of keratin 19 in A549 lung carcinoma cells [29]. Additionally, the integrated LTNP chip with NA enrichment, isolation, and digital detection functions has been developed and successfully applied to detect bovine DNA in ovine meat for food adulteration detection [72, 73].

3.3.4. Other cdNADs

Gansen et al. described a self-digitization (SD) cdLAMP device shown in **Figure 10** [32]. In this device, the reagents were partitioned into the microchambers based on an inherent fluidic phenomenon that the interplay between fluidic forces and interfacial tension could cause the self-dispersion of an income aqueous fluid into an array of chambers prefilled with an immiscible fluid. Therefore, the sample loading could be realized with manual or automated syringe pumps or external air pressure, removing the hydraulic valves or mechanical action. Less than 2 μL sample was used for the accurate quantification of relative and absolute DNA

http://dx.doi.org/10.5772/62742

concentrations. To improve the efficiency of partitioning samples, a new generation of SD chip was invented with close to 100% efficiency in 2013 [74]. In 2014, based on the SD chip, digital RT-PCR was developed to absolutely quantify mRNA from single cells [75]. Due to the simplicity and robustness of the SD chip, the SD cdNAD is an inexpensive and easy-to-operate digital detection device.

Figure 10. Design of the SD cdLAMP device. (A) Schematic diagram of the individual components of a fully assembled chip. Air pressure was delivered via a removable adapter, which was connected to an external pressure source. (B) Layout of the microfluidic network. A dense array of rectangular side chambers was connected to a thin main channel. The whole array was surrounded by a separate water reservoir to saturate the PDMS during incubation at 65°C. Scale bar, 5 mm. (C) Geometry of the side chamber array and main channel. All dimensions are in micrometers. (D) Sequential images showing the initial filling of the side-chamber array with aqueous solution. (E) Sequence of images showing the SD of aqueous sample in the side chambers. Reprinted with permission from Ref. [32]. © Copyright 2012 Royal Society of Chemistry.

In 2010, Sundberg et al. designed a spinning disk platform to achieve dPCR [25]. The disk was an inexpensive and disposable plastic disk-like chip. Differing from other approaches, 1000 nL microwells were generated by passive compartmentalization through centrifugation, and the volume of each well was 33 nL in average. The whole process, including disk loading, thermocycling, and fluorescent imaging, only costs less than 35 min. However, this kind of cdNAD performed some defects, such as the tedious plastic disk manufacturing and the probable NA adsorption to the disk.

4. Analysis and evaluation of cdNAD

This part focuses on the analysis and evaluation of cdNAD. The contents involve four aspects, which are the dehydration of microreaction, the dynamic range, the response of cdNAD, and the precision of cdNAD.

4.1. Dehydration of microreaction

In PCR, dehydration is attributable to the repeated denaturing steps, whereas, for isothermal NA amplification, reacting at a consistent temperature (e.g., 63°C) for at least 1 h results in dehydration. Also, the influence of dehydration is different according to the different material-based chips for cdNAD.

As we know, the microfluidic PDMS chips suffer from dehydration heavily. Actually, the dehydration degree is determined by the thickness of the PDMS layer between the top of the chamber and the waterproof layer. If v_f is the total volume fraction of reaction reagent, v_f is defined by the function of

$$v_f = \frac{A_{chamber} \cdot h_{chamber}}{A_{PDMS} \cdot h_{PDMS}}$$

where A and h refer to the designed area and height, respectively. Using the formula of $C_{sat\_25°C} \times P_{vap\_70°C} / P_{vap\_25°C}$, a saturated concentration of water vapor in PDMS at 70°C ($C_{sat\_70°C}$) can be calculated as 400 mol/m^3. Then, the maximum fractional loss of water (fl_{max}) from the reaction chambers is defined by

where ρ_{water} is the density of water and M_{water} is the molar mass of water.

4.2. Dynamic range

When high concentration targets are loaded, the chip panel can be completely saturated, whereas, for low targets, the chip panel still possesses the capability of realizing digital detection. Therefore, the theoretical dynamic range is determined by the high concentrations that make the chip completely saturated.

In this situation, the occurrence of an empty chamber is a small probability event, and due to statistical independence between the chamber number and the total empty chamber number, the event can be modeled as a random Poisson process. Then, the occurrence probability of t empty chamber number, $P(n=t, \lambda)$, is defined by $P(n=t, \lambda)=\lambda^t e^{-\lambda} / t!$. In the function, λ equals to the mean number of empty chambers in panels. For each empty chamber in each panel, namely, a chamber containing 0 molecule, the probability $P(n=0,\lambda)=e^{-\lambda}=e^{-m/N}$, where λ is the ratio of the loaded molecule number (m) to the chamber numbers (N). Therefore, λ is equal to the product of the probability $P(n=0,\lambda)$ and the N chamber numbers, namely, $\lambda=Ne^{-m/N}$. Finally,

$P(n=t,\ \lambda)=P\left(n=t,\ Ne^{-m/N}\right)=\left(Ne^{-m/N}\right)^{t}e^{-Ne^{-m/N}}/t!$. If λ is more than 10, the probability of the chip panel is completely saturated, P(n=0,λ)=e-10, which is less than 10-4 and can be as the acceptable failure rate. Then, $\lambda=N\,e^{-m/N}>10$, and the maximum loaded molecular number (mmax) can be calculated.

4.3. Response of cdNAD

According to the distribution of molecules across the chip, the Poisson distribution is adapted to calculate the original concentration of target stock solution.

For each chip panel, the probability (P) of having the number (n) of NA molecules per chamber is $P(n,\lambda)=(\lambda^{n}e^{-\lambda})/n!$, where λ is the ratio of loaded molecule number to chamber number of each panel. For λ, it is equal to the average molecule number per chamber, which can be expressed by the equation of $\lambda=C_0 X_{dil} V$, where C_0 is the target's original concentration, V is the volume of each chamber, and X_{dil} is the dilution factor of diluted targets used in the panel. If the stock solution is diluted in k fold, the $X_{dil}=1/k$, and particularly, the X_{dil} of stock solution is 1. When a chamber contains 0 molecule, the probability $P(n=0,\lambda)=e^{-\lambda}$. As for a chamber capturing one or more molecules, the probability $P(n\geqq 1,\lambda)=1-P(n=0,\lambda)=1-e^{-\lambda}$. After dPCR, a chamber with observed positive signal suggests that at least one target molecule is captured. Therefore, the ratio (f) of observed positive chamber number to chamber number of each panel, namely, the observed fraction of positive chambers, equals to the probability $P(n\geqq 1,\lambda)$, which is $f=P(n\geqq 1,\lambda)=1-e^{-\lambda}$. Then, $\lambda=ln(1-f)=-C_0 X_{dil} V$, and a linear variation relationship is exhibited in terms of the regression curve equation between $ln(1-f)$ and X_{dil}, because C_0 and V are constant values. Then, the target's original concentration C_0 can be calculated based on the slope of the curve ($-C_0 V$).

In addition, because the Poisson distribution is a particular case of a binomial distribution, the distribution of the positive chamber number (x) in each panel is classified as the binomial distribution. The probability distribution $P(x)$ is therefore influenced by the probability $p=P(n\geqq 1,\lambda)=1-P(n=0,\lambda)=1-e^{-\lambda}$. Based on the nature of binomial distribution, x is equal to the mean, namely, $x=Np=N(1-e^{-\lambda})$ (N, the total chamber number in each panel). Then, the average molecule number per chamber, $\lambda=ln\{N/(N-x)\}$, through which the loaded molecule number (N_e) for each panel can be estimated by the equation $N_e=N\lambda=Nln\{N/(N-x)\}$.

4.4. Precision of cdNAD

When the chamber number in each panel is very large, the Poisson distribution is approximate to normal distribution, which is also called Gaussian distribution. Use the parameters in the discussion of response and dynamic range above, and let y be a random variable representing the number of positive chambers that capture at least one molecule. Also, we can know that its mathematical expectation or mean μ is $N(1-e^{-\lambda})$, and its variance σ^2 is $Ne^{-\lambda}(1-e^{-\lambda})$. Then, the probability density function associated with y is as follows:

If the precision of cdNAD is defined as the minimum difference in concentration ($\Delta\lambda/\lambda$) that is reliably detected with more than 99% true positive and more than 99% true negative rate, this situation corresponds to 4.6σ separation in the mean (μ) for two Gaussian distributions. That is to say, in the case with small $\Delta\lambda$, $\Delta\mu/\Delta\lambda=4.6\sigma$. Then, $\partial[N(1-e^{-\lambda})]\Delta\lambda/\partial\lambda=Ne^{-\lambda}\Delta\lambda=4.6[Ne^{-\lambda}(1-e^{-\lambda})]^{1/2}$, and $\Delta\lambda/\lambda=4.6(e^{\lambda}-1)^{1/2}/(\lambda N^{1/2})$. For different total chamber numbers (N) in chip panel, the precision ($\Delta\lambda/\lambda$) to expected molecules per chamber (λ) could be plotted.

5. Application of dNAD

Compared to conventional NA detection methods, dNAD provides better sensitivity, better precision, higher tolerance, and the NA's absolute quantification. Until now, dNAD has been applied to a variety of research fields, including pathogen detection, food safety, clinical diagnosis (genetic instability estimation and early cancer), prenatal diagnosis, quantitative analysis of gene expression, and NGS library quantification. Although dPCR is still the most widespread type of dNAD, in resource-limited regions, it is confined due to the requirement of thermal cycling and robust temperature control. To overcome this awkwardness, dINAAs without thermal cycling are of great interest, which also enlarge the application of dNAD, especially for POCT. For this subchapter, the recent advances on application of dNAD will be narrated.

5.1. Pathogen detection

Honestly speaking, on pathogen detection, the advantages of most conventional NADs on both analytical sensitivity and specificity are inherited by the corresponding digital formats. In addition, dNAD has the capability of realizing NA's absolute quantification. Therefore, dNAD can be used as the ultrahigh sensitivity and more accurate method for viral load determination or bacterial quantification. Kelley et al. established a duplex ddPCR assay for high-precision methicillin-resistant *Staphylococcus aureus* (MRSA) analysis [76]. By assaying 397 clinical samples, a good agreement with the reference assay for both qPCR and ddPCR assays was indicated. Strain et al. demonstrated and estimated the application of ddPCR for a highly precise measurement of HIV DNA [77]. Total HIV DNA and episomal 2-LTR (long terminal repeat) circles in cells that were all isolated from infected patients were targeted. Compared to qPCR, ddPCR performed a significantly increased precision (5-fold for total HIV DNA and >20-fold for 2-LTR circles), making it an alternative for the measurement of HIV DNA from clinical specimens.

dNAD also enables the direct detection without NA extraction due to the ability of partitioning target NA and nontarget components (e.g., inhibitors) into different microwells. Pavšič et al. employed two dPCR platforms (QX100 ddPCR system from Bio-Rad Laboratories and the BioMark HD IFC cdPCR system from Fluidigm) for the direct quantification of two whole-virus materials of human cytomegalovirus (HCMV) without DNA extraction [78]. It was demonstrated that direct quantification by both dPCRs could provide repeatable measure-

ments of viral DNA copy numbers, giving a closer agreement with the actual viral load than that with either dPCR or qPCR of extracted DNA.

Although dNAD certainly possesses the superiority of absolute quantitation, some reports fail to demonstrate the advantage, which calls for the requirement of optimization when establishing dNAD. For instance, Boizeau et al. used ddPCR to provide an absolute quantitation of HBV genome molecules [79]. However, the results indicated that qPCR assays remained more sensitive than ddPCR when used for low HBV DNA levels, suggesting that optimization of ddPCR was still necessary, especially on accurately differentiating the positive from negative in samples with very low levels of target DNA molecules.

5.2. Food safety

Food safety mainly refers to two parts: the minoring of foodborne pathogens and the detection of GMO. For example, human noroviruses (NoV) and hepatitis A virus (HAV) are two foodborne enteric viruses that have caused the vast majority of nonbacterial gastroenteritis or some fatal infectious hepatitis. Coudray-Meunier et al. conducted a comparative study of IFC RT-cdPCR and conventional RT-qPCR when quantifying the NoV and HAV from lettuce and water samples, proving that the IFC RT-cdPCR assay was more tolerant to inhibitory substances from lettuce samples [80]. Also, the IFC RT-cdPCR may be useful for standardizing the quantification of enteric viruses in bottled water and lettuce samples. Fu et al. used the BioMark HD system equipped with a 48.770 digital array to develop cdPCR for GMO detection without pretreatment [81]. The CaMV35s promoter and the NOS terminator were selected as the targets, and nine events of GMOs (MON810, MON863, TC1507, MIR604, MIR162, GA21, T25, NK603, and Bt176) were collected to determine the specificity. The results showed that the cdPCR could achieve a discrimination of down to 0.1%, lower than the labeling threshold level of the EU, allowing highly sensitive, specific, and stable GMO screening detection. Dalmira et al. developed a duplex ddPCR assay to characterize the certified reference materials (CRMs) in terms of T-*nos*/*hmg* copy number ratio in maize [82]. After optimization using a central composite design, the duplex ddPCR method realized the absolute limit of detection (LOD) and limit of quantification (LOQ) of 11 and 23 copy number *T-nos*, namely, relative LOD of 0.034% and relative LOQ of 0.08%, respectively. The dynamic range of T-*nos*/*hmg* ratio ranged from 0.08% to 100%. The results indicated that the duplex ddPCR assay was useful for characterizing CRM candidates on T-*nos*/*hmg* ratio.

The bias caused by reliance on quantitative standards may have an impact on the results of qPCR, which is not beneficial for water monitoring and microbial source identification. Therefore, Cao et al. employed a duplex ddPCR to simultaneously quantify *Enterococcus* spp. and the human fecal-associated HF183 marker for evaluating the water quality [83]. The results demonstrated that ddPCR performed greater tolerance of inhibition than qPCR, with one to two orders of magnitude higher at inhibitor concentrations. Also, ddPCR brought about remarkably improved precision, although a lower upper LOQ than qPCR was indicated.

For food safety, it is indispensable to identify and quantify the meat products for unveiling species fraud and product mislabeling during food processing. Tian et al. used LTNP cdPCR to detect bovine meat in ovine meat [72]. Floren et al. successfully applied two-step ddPCR for

precise quantification of cattle, horse, and pig in processed meat product, with the nuclear *F2* gene targeted [84].

5.3. Clinical diagnosis

At present, clinical diagnosis including genetic instability estimation and early cancer is also the main application field for dNAD. It has been clearly confirmed that the genetic instability of human cells is one of the causes of cancer, including somatic mutation, allelic imbalance, loss of heterozygosity, CNVs, and single nucleotide variations (SNVs). Accordingly, how to discriminate the rare mutant gene from abundant normal NAs attracts great concerns of researchers. Interestingly, it is also the question that initiates the concept formation of dNAD.

As *de novo* CNV may be caused by reprogramming somatic cells into induced pluripotent stem cells, Abyzov et al. used qPCR and ddPCR to detect and estimate this phenomenon. The results showed that, in parental fibroblasts, at least half of the CNVs are indicated as low-frequency somatic genomic variants [85]. Boettger et al. successfully applied a ddPCR approach to analyze father-mother-offspring trios from HapMap at specific sites within region 1 on the investigation of inference of complex CNV and single nucleotide polymorphism (SNP) haplotypes at the human 17q21.31 locus [86].

Detecting biomarkers associated with tumor formation, development, and drug evaluations on gene expression is the useful approach for early cancer diagnosis. Up to now, various biomarkers have been identified, and dNAD reflects the unique advantage of absolute quantitation of their gene expression [87]. Zhu et al. applied SPC cdPCR to the detection of three lung cancer-related genes (PLAU, ENO2, and PLAT). cdPCR yielded comparable results to qPCR, illustrating that the established platform had the ability of realizing absolute quantitation for gene expression [30]. Floren et al. employed ddPCR to detect the BRAF-V600E and V600K mutations in melanoma circulating tumor with high sensitivity [84]. The study demonstrated that ddPCR performed 200-fold increased sensitivity than competitive allele-specific PCR (castPCR), giving an LOD of 0.0005% when combined with whole-genome amplification (WGA). Through noninvasive analysis of circulating free plasma DNA, Gevensleben et al. determined the presence of oncogenic amplification by developing a plasma DNA ddPCR assay targeting HER2 [88]. In the independent validation cohort, ddPCR could reach a positive and negative predictive value of 70% and 92%, respectively. The results suggested that ddPCR had the potential to the analysis of any locus amplified in cancer, not only in metastatic breast cancer. Beaver et al. also employed a ddPCR assay for the detection of circulating plasma tumor DNA (ptDNA) in patients with early-stage cancer [89]. A total of 30 tumors were first analyzed by Sanger sequencing for common PIK3CA mutations, and ddPCR was then used to analyze their extracted DNA for the same mutations. This ddPCR-based accurate mutation detection platform was demonstrated to be of great use for early-stage breast cancer.

As a new generation of cancer biomarkers, abnormally DNA methylation in the gene's regulatory regions can affect identical residues that may cause the cancer. The analysis of methylated genes therefore becomes more and more important in cancer research. For example, Li et al. developed a sensitive bead-based ddPCR for the quantification of DNA

methylation, which could detect down to one methylated DNA molecule in approximately 5000 unmethylated DNA molecules from plasma or fecal samples [20]. Weisenberger et al. developed an improved DNA methylation detection with single-molecule high-resolution based on IFC cdPCR and successfully identified the breast cancer-specific hypermethylation phenomenon in the CpG islands of RUNX3, CLDN5, and FOXE1 [90].

5.4. Prenatal diagnosis

Prenatal diagnosis is usually carried out by invasive or noninvasive approaches [91]. The invasive method (e.g., amniocentesis) refers to inserting needles into the uterus, which is time-consuming (several weeks required) and risky to the fetus [92]. In contrast, noninvasive method seems to be more rapid and safer. Currently, noninvasive prenatal diagnosis mainly involves ultrasonography of the womb or detecting cell-free fetal DNA (cffDNA) in maternal serum and plasma. The latter is also termed as noninvasive prenatal testing (NIPT). Appling dNAD to NIPT is the emerging noninvasive approach with high sensitivity and high precision [93–97]. Gu et al. employed the QX100 ddPCR system from Bio-Rad Laboratories to detect cffDNA for the risk of methylmalonic acidemia, confirming that ddPCR is a cost-effective and noninvasive prenatal method when diagnosing known mutations associated with Mendelian disorders [98]. Pornprasert and Prasing implemented a ddPCR for the deletion of $\alpha(0)$-thalassemia Southeast Asian (SEA)-type deletion [99]. The study showed that ddPCR might be an alternative technology to routine clinical diagnosis. Barrett et al. adopted 12×765 digital array chips to establish an IFC cdPCR to analyze the cffDNA for NIPT of sickle cell anemia [94]. The results suggested that the built IFC cdPCR is a useful method to determine the genotype of fetuses at risk for sickle cell anemia. Meantime, the report also illustrated that it was essential to optimize the fractional fetal DNA concentration.

Because most cffDNA fragments were approximately 200 bp in size and, in the early gestation, the cffDNA occupies low percentage (mostly <10%) in maternal plasma, efficient methods for the extraction of cffDNA are in great need. Holmberg et al. thereby estimated two commercial platforms to extract cffDNA: the Akonni Biosystems TruTip technology and the Circulating Nucleic Acids Kit from Qiagen [100]. Determined by QX100 ddPCR system and qPCR, the extracted products from two platforms performed similar results.

5.5. NGS library quantification

As known to all, the establishment of NGS libraries still leans mainly on manual bench-top procedures, which is slow and inefficient [101]. To solve it, Kim et al. invented an automated digital microfluidic LOC-based sample preparation for the NGS. Compared to the conventional methods, digital microfluidic LOC platform is cost-efficient and has high throughout [102]. Similarly, Thaitrong et al. integrated a droplet-based microfluidic LOC system with a unit of capillary-based reagent delivery and the quantitative CE module to develop an automated quality-control platform for NGS [103]. Besides, White et al. confirmed that dPCR is able to provide sensitive and absolute calibration for NGS, enabling direct sequencing without titration runs and with sufficient precision [11]. Fu et al. developed a picoliter-scaled droplet digital WGA (ddWGA) platform for realizing uniform and accurate single-cell

sequencing, bringing about significantly improved amplification evenness and accuracy for the simultaneous detection of CNVs and SNVs in single-cell level [104]. Weisenberger et al. applied the Fluidigm BioMark Digital Array to establish digital bisulfite genomic DNA sequencing with high resolution and high sensitivity [105]. The results showed that IFC cdPCR was a fast and reliable method for the single-molecule-scaled detection of DNA methylation information.

6. Conclusion and future prospects

Undoubtedly, there is growing interest in dNAD, because it allows the more precise NA quantification, the higher discrimination of rare NA mutants, and the more reproducible and less susceptible to inhibitors than the traditional NA methods. Consequently, dNAD has full potential to influence the development of biology research, clinical diagnosis, the safety of food and environment, and other research fields.

To enhance the impact of this promising technique and push it towards clinical application, the MIQE for dNAD (dMIQE) was also published [106]. Based on dMIQE, the experimental protocols are standardized, the efficient utilization of resources is maximized, and the data are adequately assisted. However, the promising technique of dNAD still confronts some shortcomings. On one hand, although the development of microfluidic LOC offers a lot of dNAD device platforms, these devices perform low functional integration, and the supporting detection approaches lean primarily on real-time fluorescence scanning or the endpoint analysis of CCD camera-captured images, which, to some extent, adds the real cost and also has impacts on the true detection accuracy. Therefore, in the future, it will become a general trend that dNAD devices are highly integrated with multiple functions including cell or single-cell capture, cell lysis, and NA enrichment and purification, employing more advanced supporting detection technology. Particularly, for ddNAD, the strategy of droplet generation is one of the developing directions. For instance, Tanaka et al. currently created a hands-off autonomous preparation method of monodisperse emulsion droplets using a degassed PDMS chip [107]. Jeong et al. used a specially designed three-dimensional monolithic elastomer device to create a kiloscale droplet generation [108]. According to the snap-off mechanism, Barkley et al. also invented a novel technique to generate monodisperse droplets [109].

On the other hand, dNAD is actually the digital version of NAD, thereby possessing the same disadvantages (e.g., bias or nonspecific amplification) as most sequence-based NA amplification methods. Based on this point, how to improve or guarantee the NA amplification fidelity in microreactors is one of the future prospects of dNAD. It should be noted that the optimized reaction conditions for NA amplification in microreactors might be different from those in bulk state, meaning that the optimization of reaction system is indispensable. Furthermore, the precision of dNAD is greatly influenced by the number and size of microchambers (for cdNAD) or droplet (for ddNAD), which in turn challenges the fabrication of microfluidic chip and the uniformity of partitioning. Accordingly, we also anticipate that, in the future, there will be some novel strategies developed to realize digital detection not only based on partitioning reagents.

Certainly, the application of dNAD will be enlarged by combining with other molecular assays, especially for single-cell analysis and single-cell genomic sequencing. For example, dNAD can combine with proximity ligation or PEAs to achieve single-molecule protein biomarker detection. Additionally, in the future, ongoing comparison tests of dNAD and qPCR will roundly prove the detection superiority of dNAD in many research fields. Also, dNAD will become the promising POCT-oriented research area for the ambitious plan of precision medicine.

Conclusively, dNAD based on microfluidic LOC devices will continue to provide further opportunities for determining NA molecules, protein molecules, and other biomolecules towards deep analysis with high sensitivity and precision.

Author details

Xiong Ding[1,2] and Ying Mu[1*]

*Address all correspondence to: muying@zju.edu.cn

1 Research Center for Analytical Instrumentation, Institute of Cyber-Systems and Control, State Key Laboratory of Industrial Control Technology, Zhejiang University, Hangzhou, P.R. China

2 College of Life Sciences, Zhejiang University, Hangzhou, P.R. China

References

[1] Biomarkers SMAPN, Gilad S, Meiri E, Yogev Y, Benjamin S, Lebanony D, et al. Serum microRNAs are promising novel biomarkers. PLoS ONE. 2008;3(9):e3148.

[2] Blakely WF. Nucleic acid molecular biomarkers for diagnostic biodosimetry applications: use of the fluorogenic 5′-nuclease polymerase chain reaction assay. Military Medicine. 2002;167(2):16–19.

[3] Chen X, Ba Y, Ma L, Cai X, Yin Y, Wang K, et al. Characterization of microRNAs in serum: a novel class of biomarkers for diagnosis of cancer and other diseases. Cell Research. 2008;18(10):997–1006.

[4] Schwarzenbach H, Hoon DS, Pantel K. Cell-free nucleic acids as biomarkers in cancer patients. Nature Reviews Cancer. 2011;11(6):426–437.

[5] Tost J. DNA methylation: an introduction to the biology and the disease-associated changes of a promising biomarker. Molecular Biotechnology. 2010;44(1):71–81.

[6] Chen Y, Perkins M, Teixeira L, Cave M, Eisenach K. Comparison of the ABI 7700 system (TaqMan) and competitive PCR for quantification of IS6110 DNA in sputum during treatment of tuberculosis. Journal of Clinical Microbiology. 1998;36(7):1964–1968.

[7] Tobal K, Newton J, Macheta M, Chang J, Morgenstern G, Evans P, et al. Molecular quantitation of minimal residual disease in acute myeloid leukemia with t(8;21) can identify patients in durable remission and predict clinical relapse. Blood. 2000;95(3): 815–819.

[8] Gack MU, Kirchhofer A, Shin YC, Inn K-S, Liang C, Cui S, et al. Roles of RIG-I N-terminal tandem CARD and splice variant in TRIM25-mediated antiviral signal transduction. Proceedings of the National Academy of Sciences. 2008;105(43):16743–16748.

[9] Neely LA, Patel S, Garver J, Gallo M, Hackett M, McLaughlin S, et al. A single-molecule method for the quantitation of microRNA gene expression. Nature Methods. 2006;3(1): 41–46.

[10] Jarvius J, Melin J, Göransson J, Stenberg J, Fredriksson S, Gonzalez-Rey C, et al. Digital quantification using amplified single-molecule detection. Nature Methods. 2006;3(9): 725–727.

[11] White RA, Blainey PC, Fan HC, Quake SR. Digital PCR provides sensitive and absolute calibration for high throughput sequencing. BMC Genomics. 2009;10(1):116.

[12] Shiroguchi K, Jia TZ, Sims PA, Xie XS. Digital RNA sequencing minimizes sequence-dependent bias and amplification noise with optimized single-molecule barcodes. Proceedings of the National Academy of Sciences. 2012;109(4):1347–1352.

[13] Shuga J, Zeng Y, Novak R, Lan Q, Tang X, Rothman N, et al. Single molecule quantitation and sequencing of rare translocations using microfluidic nested digital PCR. Nucleic Acids Research. 2013:41(16):e159.

[14] Pfaffl MW. A new mathematical model for relative quantification in real-time RT-PCR. Nucleic Acids Research. 2001;29(9):e45–e45.

[15] Čikoš Š, Bukovská A, Koppel J. Relative quantification of mRNA: comparison of methods currently used for real-time PCR data analysis. BMC Molecular Biology. 2007;8(1):113.

[16] Whelan JA, Russell NB, Whelan MA. A method for the absolute quantification of cDNA using real-time PCR. Journal of Immunological Methods. 2003;278(1):261–269.

[17] Bustin SA. Absolute quantification of mRNA using real-time reverse transcription polymerase chain reaction assays. Journal of Molecular Endocrinology. 2000;25(2):169–193.

[18] Schmittgen TD, Livak KJ. Analyzing real-time PCR data by the comparative CT method. Nature Protocols. 2008;3(6):1101–1108.

[19] Zachar V, Thomas RA, Goustin AS. Absolute quantification of target DNA: a simple competitive PCR for efficient analysis of multiple samples. Nucleic Acids Research. 1993;21(8):2017.

[20] Li M, Chen W-d, Papadopoulos N, Goodman SN, Bjerregaard NC, Laurberg S, et al. Sensitive digital quantification of DNA methylation in clinical samples. Nature Biotechnology. 2009;27(9):858–863.

[21] Fu GK, Wilhelmy J, Stern D, Fan HC, Fodor SP. Digital encoding of cellular mRNAs enabling precise and absolute gene expression measurement by single-molecule counting. Analytical Chemistry. 2014;86(6):2867–2870.

[22] Whale AS, Cowen S, Foy CA, Huggett JF. Methods for applying accurate digital PCR analysis on low copy DNA samples. PLoS ONE. 2013;8(3):e58177.

[23] Vogelstein B, Kinzler KW. Digital PCR. Proceedings of the National Academy of Sciences. 1999;96(16):9236–9241.

[24] Men Y, Fu Y, Chen Z, Sims PA, Greenleaf WJ, Huang Y. Digital polymerase chain reaction in an array of femtoliter polydimethylsiloxane microreactors. Analytical Chemistry. 2012;84(10):4262–4266.

[25] Sundberg SO, Wittwer CT, Gao C, Gale BK. Spinning disk platform for microfluidic digital polymerase chain reaction. Analytical Chemistry. 2010;82(4):1546–1550.

[26] Shen F, Du W, Kreutz JE, Fok A, Ismagilov RF. Digital PCR on a SlipChip. Lab on a Chip. 2010;10(20):2666–2672.

[27] Fan HC, Blumenfeld YJ, El-Sayed YY, Chueh J, Quake SR. Microfluidic digital PCR enables rapid prenatal diagnosis of fetal aneuploidy. American Journal of Obstetrics and Gynecology. 2009;200(5):e541–543, e547.

[28] Pinheiro LB, Coleman VA, Hindson CM, Herrmann J, Hindson BJ, Bhat S, et al. Evaluation of a droplet digital polymerase chain reaction format for DNA copy number quantification. Analytical Chemistry. 2011;84(2):1003–1011.

[29] Tian Q, Song Q, Xu Y, Zhu Q, Yu B, Jin W, et al. A localized temporary negative pressure assisted microfluidic device for detecting keratin 19 in A549 lung carcinoma cells with digital PCR. Analytical Methods. 2015;7(5):2006–2011.

[30] Zhu Q, Qiu L, Yu B, Xu Y, Gao Y, Pan T, et al. Digital PCR on an integrated self-priming compartmentalization chip. Lab on a Chip. 2014;14(6):1176–1185.

[31] Zhu Q, Gao Y, Yu B, Ren H, Qiu L, Han S, et al. Self-priming compartmentalization digital LAMP for point-of-care. Lab on a Chip. 2012;12(22):4755–4763.

[32] Gansen A, Herrick AM, Dimov IK, Lee LP, Chiu DT. Digital LAMP in a sample self-digitization (SD) chip. Lab on a Chip. 2012;12(12):2247–2254.

[33] Blainey PC, Quake SR. Digital MDA for enumeration of total nucleic acid contamination. Nucleic Acids Research. 2011;39(4):e19–e19.

[34] Shen F, Davydova EK, Du W, Kreutz JE, Piepenburg O, Ismagilov RF. Digital isothermal quantification of nucleic acids via simultaneous chemical initiation of recombinase polymerase amplification reactions on SlipChip. Analytical Chemistry. 2011;83(9): 3533–3540.

[35] Mazutis L, Araghi AF, Miller OJ, Baret J-C, Frenz L, Janoshazi A, et al. Droplet-based microfluidic systems for high-throughput single DNA molecule isothermal amplification and analysis. Analytical Chemistry. 2009;81(12):4813–4821.

[36] Rane TD, Chen L, Zec HC, Wang T-H. Microfluidic continuous flow digital loop-mediated isothermal amplification (LAMP). Lab on a Chip. 2015;15(3):776–782.

[37] Schuler F, Schwemmer F, Trotter M, Wadle S, Zengerle R, von Stetten F, et al. Centrifugal step emulsification applied for absolute quantification of nucleic acids by digital droplet RPA. Lab on a Chip. 2015;15(13):2759–2766

[38] Konry T, Smolina I, Yarmush JM, Irimia D, Yarmush ML. Ultrasensitive detection of low-abundance surface-marker protein using isothermal rolling circle amplification in a microfluidic nanoliter platform. Small. 2011;7(3):395–400.

[39] Pohl G, Shih I-M. Principle and applications of digital PCR. Expert Rev Mol Diagn. 2004;4(1):41–47.

[40] Barrett AN, Chitty LS. Developing noninvasive diagnosis for single-gene disorders: the role of digital PCR. Methods in Molecular Biology. 2014;1160:215–228.

[41] Lo YD, Lun FM, Chan KA, Tsui NB, Chong KC, Lau TK, et al. Digital PCR for the molecular detection of fetal chromosomal aneuploidy. Proceedings of the National Academy of Sciences. 2007;104(32):13116–13121.

[42] Baker M. Digital PCR hits its stride. Nature Methods. 2012;9(6):541–544.

[43] Morrison T, Hurley J, Garcia J, Yoder K, Katz A, Roberts D, et al. Nanoliter high throughput quantitative PCR. Nucleic Acids Research. 2006;34(18):e123–e123.

[44] Marx V. PCR: paths to sensitivity. Nature Methods. 2014;11(3):241–245.

[45] Majumdar N, Wessel T, Marks J. Digital PCR modeling for maximal sensitivity, dynamic range and measurement precision. PLoS ONE. 2015;10(3):e0118833.

[46] Conte D, Verri C, Borzi C, Suatoni P, Pastorino U, Sozzi G, et al. Novel method to detect microRNAs using chip-based QuantStudio 3D digital PCR. BMC Genomics. 2015;16(1): 1.

[47] Klančnik A, Toplak N, Kovač M, Marquis H, Jeršek B. Quantification of *Listeria monocytogenes* cells with digital PCR and their biofilm cells with real-time PCR. Journal of Microbiological Methods. 2015;118:37–41.

[48] Kinz E, Leiherer A, Lang A, Drexel H, Muendlein A. Accurate quantitation of JAK2 V617F allele burden by array-based digital PCR. International Journal of Laboratory Hematology. 2015;37(2):217–224.

[49] Kaitu'u-Lino T, Hastie R, Cannon P, Lee S, Stock O, Hannan NJ, et al. Stability of absolute copy number of housekeeping genes in preeclamptic and normal placentas, as measured by digital PCR. Placenta. 2014;35(12):1106–1109.

[50] Schweitzer P, Harris A, Mandelman D, Jackson S, Cifuentes F, Degoricija L. Precise quantification of next generation sequencing Ion Torrent™ and Illumina Libraries using the QuantStudio™ 3D Digital PCR Platform. Journal of Biomolecular Techniques. 2014;25(Suppl):S15.

[51] Leng X, Zhang W, Wang C, Cui L, Yang CJ. Agarose droplet microfluidics for highly parallel and efficient single molecule emulsion PCR. Lab on a Chip. 2010;10(21):2841–2843.

[52] Kennedy, Suzanne. PCR troubleshooting and optimization: the essential guide. Horizon Scientific Press, 2011.

[53] Williams R, Peisajovich SG, Miller OJ, Magdassi S, Tawfik DS, Griffiths AD. Amplification of complex gene libraries by emulsion PCR. Nature Methods. 2006;3(7):545–550.

[54] Tavvfik DS, Griffiths AD. Man-made cell-like compartments for molecular evolution. Nature Biotechnology. 1998;16(7):652–656

[55] Margulies M, Egholm M, Altman WE, Attiya S, Bader JS, Bemben LA, et al. Genome sequencing in microfabricated high-density picolitre reactors. Nature. 2005;437(7057): 376–380.

[56] Selck DA, Karymov MA, Sun B, Ismagilov RF. Increased robustness of single-molecule counting with microfluidics, digital isothermal amplification, and a mobile phone versus real-time kinetic measurements. Analytical Chemistry. 2013;85(22):11129–11136.

[57] Beer NR, Wheeler EK, Lee-Houghton L, Watkins N, Nasarabadi S, Hebert N, et al. On-chip single-copy real-time reverse-transcription PCR in isolated picoliter droplets. Analytical Chemistry. 2008;80(6):1854–1858.

[58] Zhong Q, Bhattacharya S, Kotsopoulos S, Olson J, Taly V, Griffiths AD, et al. Multiplex digital PCR: breaking the one target per color barrier of quantitative PCR. Lab on a Chip. 2011;11(13):2167–2174.

[59] Hindson BJ, Ness KD, Masquelier DA, Belgrader P, Heredia NJ, Makarewicz AJ, et al. High-throughput droplet digital PCR system for absolute quantitation of DNA copy number. Analytical Chemistry. 2011;83(22):8604–8610.

[60] Liu W, Chen D, Du W, Nichols KP, Ismagilov RF. SlipChip for immunoassays in nanoliter volumes. Analytical Chemistry. 2010;82(8):3276–3282.

[61] Li L, Ismagilov RF. Protein crystallization using microfluidic technologies based on valves, droplets, and SlipChip. Biophysics. 2010;39:139–158

[62] Shen F, Du W, Davydova EK, Karymov MA, Pandey J, Ismagilov RF. Nanoliter multiplex PCR arrays on a SlipChip. Analytical Chemistry. 2010;82(11):4606–4612.

[63] Sun B, Shen F, McCalla SE, Kreutz JE, Karymov MA, Ismagilov RF. Mechanistic evaluation of the pros and cons of digital RT-LAMP for HIV-1 viral load quantification on a microfluidic device and improved efficiency via a two-step digital protocol. Analytical Chemistry. 2013;85(3):1540–1546.

[64] Xia Y, Liu Z, Yan S, Yin F, Feng X, Liu B-F. Identifying multiple bacterial pathogens by loop-mediated isothermal amplification on a rotate & react slipchip. Sensors and Actuators B: Chemical. 2016;228:491–499.

[65] Unger MA, Chou H-P, Thorsen T, Scherer A, Quake SR. Monolithic microfabricated valves and pumps by multilayer soft lithography. Science. 2000;288(5463):113–116.

[66] Ottesen EA, Hong JW, Quake SR, Leadbetter JR. Microfluidic digital PCR enables multigene analysis of individual environmental bacteria. Science. 2006;314(5804):1464–1467.

[67] Heyries KA, Tropini C, VanInsberghe M, Doolin C, Petriv I, Singhal A, et al. Megapixel digital PCR. Nature Methods. 2011;8(8):649–651.

[68] Xu L, Lee H, Jetta D, Oh KW. Vacuum-driven power-free microfluidics utilizing the gas solubility or permeability of polydimethylsiloxane (PDMS). Lab on a Chip. 2015;15(20):3962–3979.

[69] Song Q, Gao Y, Zhu Q, Tian Q, Yu B, Song B, et al. A nanoliter self-priming compartmentalization chip for point-of-care digital PCR analysis. Biomedical Microdevices. 2015;17(3):1–8.

[70] Ding X, Wu W, Zhu Q, Zhang T, Jin W, Mu Y. Mixed-dye-based label-free and sensitive dual fluorescence for the product detection of nucleic acid isothermal multiple-self-matching-initiated amplification. Analytical Chemistry. 2015;87(20):10306–10314.

[71] Ding X, Nie K, Shi L, Zhang Y, Guan L, Zhang D, et al. Improved detection limit in rapid detection of human enterovirus 71 and coxsackievirus A16 by a novel reverse transcription-isothermal multiple-self-matching-initiated amplification assay. Journal of Clinical Microbiology. 2014;52(6):1862–1870.

[72] Tian Q, Mu Y, Xu Y, Song Q, Yu B, Ma C, et al. An integrated microfluidic system for bovine DNA purification and digital PCR detection. Analytical Biochemistry. 2015;491:55–57.

[73] Tian Q, Yu B, Mu Y, Xu Y, Ma C, Zhang T, et al. An integrated temporary negative pressure assisted microfluidic chip for DNA isolation and digital PCR detection. RSC Advances. 2015;5(100):81889–81896.

[74] Schneider T, Yen GS, Thompson AM, Burnham DR, Chiu DT. Self-digitization of samples into a high-density microfluidic bottom-well array. Analytical Chemistry. 2013;85(21):10417–10423.

[75] Thompson AM, Gansen A, Paguirigan AL, Kreutz JE, Radich JP, Chiu DT. Self-digitization microfluidic chip for absolute quantification of mRNA in single cells. Analytical Chemistry. 2014;86(24):12308–12314.

[76] Kelley K, Cosman A, Belgrader P, Chapman B, Sullivan DC. Detection of methicillin-resistant *Staphylococcus aureus* by a duplex droplet digital PCR assay. Journal of Clinical Microbiology. 2013;51(7):2033–2039.

[77] Strain MC, Lada SM, Luong T, Rought SE, Gianella S, Terry VH, et al. Highly precise measurement of HIV DNA by droplet digital PCR. PLoS ONE. 2013;8(4):e55943.

[78] Pavšič J, Žel J, Milavec M. Digital PCR for direct quantification of viruses without DNA extraction. Analytical and Bioanalytical Chemistry. 2016;408(1):67–75.

[79] Boizeau L, Laperche S, Désiré N, Jourdain C, Thibault V, Servant-Delmas A. Could droplet digital PCR be used instead of real-time PCR for quantitative detection of the hepatitis B virus genome in plasma? Journal of Clinical Microbiology. 2014;52(9):3497–3498.

[80] Coudray-Meunier C, Fraisse A, Martin-Latil S, Guillier L, Delannoy S, Fach P, et al. A comparative study of digital RT-PCR and RT-qPCR for quantification of hepatitis A virus and norovirus in lettuce and water samples. International Journal of Food Microbiology. 2015;201:17–26.

[81] Fu W, Zhu P, Wang C, Huang K, Du Z, Tian W, et al. A highly sensitive and specific method for the screening detection of genetically modified organisms based on digital PCR without pretreatment. Scientific Reports. 2015; 5:12715. doi:10.1038/srep12715.

[82] Dalmira Fl-Ud, Melina Pr-U, José-Benigno VT, Josefina Ln-Fl, Raymundo Ga-E, Abraham A-S. Development, optimization, and evaluation of a duplex droplet digital PCR assay to quantify the T-nos/hmg copy number ratio in genetically modified maize. Analytical Chemistry. 2015;88(1):812–819.

[83] Cao Y, Raith MR, Griffith JF. Droplet digital PCR for simultaneous quantification of general and human-associated fecal indicators for water quality assessment. Water Research. 2015;70:337–349.

[84] Floren C, Wiedemann I, Brenig B, Schütz E, Beck J. Species identification and quantification in meat and meat products using droplet digital PCR (ddPCR). Food Chemistry. 2015;173:1054–1058.

[85] Abyzov A, Mariani J, Palejev D, Zhang Y, Haney MS, Tomasini L, et al. Somatic copy number mosaicism in human skin revealed by induced pluripotent stem cells. Nature. 2012;492(7429):438–442.

[86] Boettger LM, Handsaker RE, Zody MC, McCarroll SA. Structural haplotypes and recent evolution of the human 17q21. 31 region. Nature Genetics. 2012;44(8):881–885.

[87] Day E, Dear PH, McCaughan F. Digital PCR strategies in the development and analysis of molecular biomarkers for personalized medicine. Methods. 2013;59(1):101–107.

[88] Gevensleben H, Garcia-Murillas I, Graeser MK, Schiavon G, Osin P, Parton M, et al. Noninvasive detection of HER2 amplification with plasma DNA digital PCR. Clinical Cancer Research. 2013;19(12):3276–3284.

[89] Beaver JA, Jelovac D, Balukrishna S, Cochran R, Croessmann S, Zabransky D, et al. Detection of cancer DNA in plasma of early stage breast cancer patients. Clinical Cancer Research. 20(10):2643–50.

[90] Weisenberger DJ, Liang G. Contributions of DNA methylation aberrancies in shaping the cancer epigenome. Translational Cancer Research. 2015;4(3):219–234.

[91] Collins S, Impey L. Prenatal diagnosis: types and techniques. Early Human Development. 2012;88(1):3–8.

[92] Young C, von Dadelszen P, Alfirevic Z. Instruments for chorionic villus sampling for prenatal diagnosis (review). Cochrane Database of Systematic Reviews. 2013;1:CD000114.

[93] Debrand E, Lykoudi A, Bradshaw E, Allen SK. A non-invasive droplet digital PCR (ddPCR) assay to detect paternal CFTR mutations in the cell-free fetal DNA (cffDNA) of three pregnancies at risk of cystic fibrosis via compound heterozygosity. PLoS ONE. 2015;10(11):e0142729.

[94] Barrett AN, McDonnell TC, Chan KA, Chitty LS. Digital PCR analysis of maternal plasma for noninvasive detection of sickle cell anemia. Clinical Chemistry. 2012;58(6): 1026–1032.

[95] Svobodová I, Pazourková E, Hořínek A, Novotná M, Calda P, Korabečná M. Performance of droplet digital PCR in non-invasive fetal RHD genotyping—comparison with a routine real-time PCR based approach. PLoS ONE. 2015;10(11):e0142572.

[96] Jin S, Lin XM, Law H, Kwek KY, Yeo GS, Ding C. Further improvement in quantifying male fetal DNA in maternal plasma. Clinical Chemistry. 2012;58(2):465–468.

[97] Kantak C, Chang C-P, Wong CC, Mahyuddin A, Choolani M, Rahman A. Lab-on-a-Chip technology: impacting non-invasive prenatal diagnostics (NIPD) through miniaturisation. Lab on a Chip. 2014;14(5):841–854.

[98] Gu W, Koh W, Blumenfeld YJ, El-Sayed YY, Hudgins L, Hintz SR, et al. Noninvasive prenatal diagnosis in a fetus at risk for methylmalonic acidemia. Genetics in Medicine. 2014;16(7):564–567.

[99] Pornprasert S, Prasing W. Detection of α(0)-thalassemia South-East Asian-type deletion by droplet digital PCR. European Journal of Haematology. 2014;92(3):244–248.

[100] Holmberg RC, Gindlesperger A, Stokes T, Lopez D, Hyman L, Freed M, et al. Akonni TruTip® and Qiagen® methods for extraction of fetal circulating DNA—evaluation by real-time and digital PCR. PLoS ONE. 2013;8(8):e73068.

[101] Voelkerding KV, Dames SA, Durtschi JD. Next-generation sequencing: from basic research to diagnostics. Clinical Chemistry. 2009;55(4):641–658.

[102] Kim H, Jebrail MJ, Sinha A, Bent ZW, Solberg OD, Williams KP, et al. A microfluidic DNA library preparation platform for next-generation sequencing. PLoS ONE. 2013;8(7):e68988.

[103] Thaitrong N, Kim H, Renzi RF, Bartsch MS, Meagher RJ, Patel KD. Quality control of next-generation sequencing library through an integrative digital microfluidic platform. Electrophoresis. 2012;33(23):3506–3513.

[104] Fu Y, Li C, Lu S, Zhou W, Tang F, Xie XS, et al. Uniform and accurate single-cell sequencing based on emulsion whole-genome amplification. Proceedings of the National Academy of Sciences. 2015;112(38):11923–11928.

[105] Weisenberger DJ, Trinh BN, Campan M, Sharma S, Long TI, Ananthnarayan S, et al. DNA methylation analysis by digital bisulfite genomic sequencing and digital MethyLight. Nucleic Acids Research. 2008;36(14):4689–4698.

[106] Huggett JF, Foy CA, Benes V, EMSLie K, Garson JA, Haynes R, et al. The digital MIQE guidelines: minimum information for publication of quantitative digital PCR experiments. Clinical Chemistry. 2013;59(6):892–902.

[107] Tanaka H, Yamamoto S, Nakamura A, Nakashoji Y, Okura N, Nakamoto N, et al. Hands-off preparation of monodisperse emulsion droplets using a poly (dimethylsiloxane) microfluidic chip for droplet digital PCR. Analytical Chemistry. 2015;87(8): 4134–4143.

[108] Jeong H-H, Yelleswarapu VR, Yadavali S, Issadore D, Lee D. Kilo-scale droplet generation in three-dimensional monolithic elastomer device (3D MED). Lab on a Chip. 2015;15(23):4387–4392.

[109] Barkley S, Weeks ER, Dalnoki-Veress K. Snap-off production of monodisperse droplets. European Physical Journal E. 2015;38(12):1–4.

IntechOpen